DE GRUYTER Open Physics 2025; 23: 20250134

Research Article

Maroua Amel Boubekeur, İrem Akbulut Arik, and Seda Igret Araz*

Theoretical and numerical investigation of a memristor system with a piecewise memductance under fractal–fractional derivatives

https://doi.org/10.1515/phys-2025-0134
received November 11, 2024; accepted January 10, 2025

Abstract: This research deals with the theoretical and numerical investigations of a memristor system with memductance function. Stability, dissipativity, and Lyapunov exponents are extensively investigated and the chaotic tendencies of the system are studied in depth. The memristor model, where a piecewise memductance function is incorporated, is modified with fractal–fractional derivatives with exponential decay, power law, and Mittag–Leffler kernels, which provide powerful tools for modeling complex systems with memory effects, long-range interactions, and fractal-like behavior. Employing the Krasnoselskii–Krein uniqueness theorem and the fixed point theorem, the existence and uniqueness of the solutions of the model including fractal–fractional derivatives with the Mittag–Leffler kernel are proven. The fractal–fractional derivative model is solved numerically using the Lagrange polynomial approach, and the chaotic tendencies of the system are exhibited through numerical simulations. The findings indicated that the memristor model with fractal–fractional derivatives was observed to exhibit chaotic behavior.

Keywords: memristor system, piecewise memductance function, fractal–fractional derivatives, Krasnoselskii–Krein uniqueness theorem

*** Corresponding author: Seda Igret Araz,** Department of Mathematic Education, Faculty of Education, Siirt University, Siirt, Turkey, e-mail: sedaaraz@siirt.edu.tr
Maroua Amel Boubekeur: Department of Mathematics and Computer Science, University of Mostaganem, Mostaganem, Algeria
İrem Akbulut Arik: Department of Mathematic Education, Faculty of Education, Siirt University, Siirt, Turkey

1 Introduction

Incorporating fractal and fractional properties into memristors can significantly increase their potential. These models aim to account for the complex, self-similarity behaviors in certain phenomena that are not captured by traditional memristor, which typically rely on integer-order differential equations. Fractals are geometric structures characterized by self-similarity, meaning their structure appears similar at any scale. In terms of memristors, fractal-based models could be used to represent devices where the internal state changes at different scales or exhibit multi-scale dynamics. For instance, the device's current–voltage curve might exhibit repeating or scaling behaviors across different ranges. The internal memory states of the device could have multi-scale, fractal-like structures that enable more complex memory behavior. When applied to memristors, fractional dynamics could be described as follows [1–3]. Memristors with fractional-order dynamics would exhibit non-exponential memory decay or recovery, capturing more realistic behaviors found in real-world materials that show non-local memory effects. The resistance of the memristor could change according to fractional powers or integrals of time, voltage, or charge. This could model complex, non-linear resistance switching characteristics seen in advanced memory devices. The concept of fractal–fractional derivative made a significant contribution to the literature by combining these two concepts. A memristor with fractal–fractional properties would exhibit a more complex and versatile set of behaviors, offering potential advantages in various fields like non-volatile memory, artificial intelligence, and modeling of complex physical systems. By incorporating fractional calculus and fractal geometry into the traditional memristor model, researchers could create new devices and technologies with enhanced performance and capabilities [4–12].

The memristor, also known as a memory resistor, is a recently discovered passive circuit component with two terminals. In 1971, Dr. Leon Chua proposed the assumption of introducing a new circuit element that has a relationship between its flux and charge, in addition to the resistor, inductor, and capacitor. Memristor and memristor systems play a crucial role in various fields including computer architecture, electronics, signal processing, image processing, programmable logic circuits, filter circuits, and communication electronics systems. Expected to revolutionize multiple domains, there are several models of the memristor discussed in the literature. Bao *et al.* [4] conducted research into the dynamic behaviors of the new smooth memristor oscillator with the variations in circuit parameters and initial conditions. Apollos discusses mathematical models of memristors, including linear, non-linear, exponential, Simmons tunnel barrier, and TEAM models. Various window functions are explored for modeling memristor behavior. These models help understand the relationship between voltage and current in memristors for potential applications in computing and electronics [5]. Radwan et al. proposed a mathematical model for memristors with linear dopant drift, matching SPICE simulations. They derived frequency response, pinched i–v hysteresis fundamentals, and analyzed resistance models, including comparisons and peak current analysis [6]. Elgabra et al. proposed a modified exponential model for memristor device modeling, enhancing memory design. They compared linear, nonlinear, and exponential models, highlighting the superior performance of the exponential model [7]. Abro and Atangana proposed a novel mathematical model based on a fifth-order chaotic circuit with two memristors, discussing chaotic behavior under varying fractal and fractional orders using numerical schemes [8]. The article presents a generalized mathematical model of memristor to confirm its characteristics. The model includes HP memristor, piecewise-linear memristor, and others as special cases. Sun et al. proposed a model to distinguish memristors from other mathematical models, enhancing reliability in identifying memristors through simulations [9]. The objective of this study is to analyze the outputs of a modified memristor system, in which the memductance function is taken as a piecewise function and fractal–fractional derivatives are employed.

Now, we present some definitions of the fractal–fractional derivatives with power law, exponential decay, and Mittag–Leffler kernels [13–17]. The fractal derivative introduced in the study by Chen [14] is defined by

$$\frac{\mathrm{d}}{\mathrm{d}t^{\beta}}w(t) = \lim_{t\to t_1}\frac{w(t) - w(t_1)}{t^{\beta} - t_1^{\beta}}, \tag{1}$$

where $\beta > 0$. The fractal–fractional derivative with exponential decay kernel of the function $\omega(t)$ is represented by [13]

$${}^{\mathrm{FFE}}_{0}D_t^{\alpha,\beta}\omega(t) = \frac{1}{1-\alpha}\frac{\mathrm{d}}{\mathrm{d}t^{\beta}}\int_0^t \omega(\zeta)\exp\left[-\frac{\alpha}{1-\alpha}(t-\zeta)\right]\mathrm{d}\zeta, \tag{2}$$

where $0 < \alpha, \beta \le 1$. The associated integral is given by

$${}^{\mathrm{FFE}}_{0}J_t^{\alpha,\beta}\omega(t) = (1-\alpha)\beta t^{\beta-1}\omega(t) + \alpha\beta\int_0^t \zeta^{\beta-1}\omega(\zeta)\mathrm{d}\zeta. \tag{3}$$

The fractal–fractional derivative with power-law of the function $\omega(t)$ is defined by [13]

$${}^{\mathrm{FFP}}_{0}D_t^{\alpha,\beta}\omega(t) = \frac{1}{\Gamma(1-\alpha)}\frac{\mathrm{d}}{\mathrm{d}t^{\beta}}\int_0^t \omega(\zeta)(t-\zeta)^{-\alpha}\mathrm{d}\zeta, \tag{4}$$

where $0 < \alpha, \beta \le 1$. The associated integral is represented by

$${}^{\mathrm{FFP}}_{0}J_t^{\alpha,\beta}\omega(t) = \frac{\beta}{\Gamma(\alpha)}\int_0^t \zeta^{\beta-1}\omega(\zeta)(t-\zeta)^{\alpha-1}\mathrm{d}\zeta. \tag{5}$$

The fractal–fractional derivative with Mittag–Leffler kernel of the function $\omega(t)$ is defined as [13]

$${}^{\mathrm{FFM}}_{0}D_t^{\alpha,\beta}\omega(t) = \frac{1}{1-\alpha}\frac{\mathrm{d}}{\mathrm{d}t^{\beta}}\int_0^t \omega(\zeta)E_{\alpha}\left[-\frac{\alpha}{1-\alpha}(t-\zeta)^{\alpha}\right]\mathrm{d}\zeta, \tag{6}$$

where $0 < \alpha, \beta \le 1$. The associated integral is given by

$$\begin{aligned}{}^{\mathrm{FFM}}_{0}J_t^{\alpha,\beta}\omega(t) &= (1-\alpha)\beta t^{\beta-1}\omega(t)\\ &\quad + \frac{\alpha\beta}{\Gamma(\alpha)}\int_0^t \zeta^{\beta-1}\omega(\zeta)(t-\zeta)^{\alpha-1}\mathrm{d}\zeta.\end{aligned} \tag{7}$$

Now, we present some Banach and Krasnoselskii's fixed point theorem.

Lemma 1.1. (Banach's fixed point theorem) *Assume X is a Banach space, and $D \subset X$, D is a closed subset. If the operator $Q : D \to D$ holds the contraction condition, then Q has a unique fixed point in D.*

Lemma 1.2. (Krasnoselskii's fixed point theorem [18]) *Assume D is a closed convex nonempty subset of a Banach space X. Assume Q and P are two operators such that*

(i) *$Qu + Pv \in D$, whenever $u, v \in D$;*
(ii) *P is compact and continuous;*
(iii) *Q is contraction mapping. Then, there exists $w \in D$ such that $z = Qw + Pw$.*

2 Memristor system

The need for memristors arises from their unique advantages in modern electronics. For instance, the memristor is beneficial for low-power computation and storage, enabling data retention without power. This characteristic is crucial for developing energy-efficient devices, as it reduces power consumption and extends battery life. Additionally, the memristor's nonlinear properties and memory characteristics make it ideal for designing chaotic circuits, advanced memory devices, and neural networks. These applications are essential for the advancement of artificial intelligence and machine learning, as they allow for more efficient and powerful computing architectures. Thus, incorporating memristors into electronic systems can lead to significant improvements in performance and energy efficiency [12].

The memristor system introduced by Bao *et al.* [4] is the focus of this section. The associated model under investigation is represented by the following system:

$$\begin{cases} \dot{x}(t) = \alpha_1(y - x + \xi x - W(w)x) \\ \dot{y}(t) = x - y + z \\ \dot{z}(t) = -\beta_1 y - \gamma z \\ \dot{w}(t) = x, \end{cases} \tag{8}$$

where the function $W(w) = \frac{\mathrm{d}}{\mathrm{d}t}(aw + bw^3) = a + 3bw^2$ is the memductance function. The functions x, y, z, and w describe two capacitors, the inductor, and the memristor, respectively.

The descriptions of the parameters of the model are presented in Table 1.

We will now present the numerical simulations for the considered memristor model by using the parameter values in Table 1 and the following initial data:

$$x(0) = 0.001, y(0) = 0.001, z(0) = 0.001, w(0) = 0.001.$$

The numerical simulations for memristor system are performed in Figure 1.

Table 1: Descriptions of the parameters of the model

Parameter	Description	Value
α_1	The reciprocal of capacitance	16.4
ξ	Conductance	1.4
β_1	The reciprocal of inductance	15
γ	The ratio of resistance to inductance	0.5
a	Positive constant of cubic function	0.2
b	Positive constant of cubic function	0.4

2.1 Some analysis of the considered memristor system

This section provides some analyses including equilibrium points, stability analysis, Lyapunov exponents, and dimension for the memristor system presented earlier [4].

2.1.1 Equilibrium point and stability analysis

We start our analysis with obtaining the equilibrium point. To achieve our aim, we need to solve the following system:

$$\begin{aligned} \alpha_1(y - x + \xi x - W(w)x) &= 0, \\ x - y + z &= 0, \\ -\beta_1 y - \gamma z &= 0, \\ x &= 0. \end{aligned} \tag{9}$$

Then, the equilibrium point is calculated as

$$E = (0,\ 0,\ 0,\ \xi), \tag{10}$$

where ξ is a constant.

The Jacobian matrix is a powerful tool for analyzing the stability of equilibrium points in nonlinear systems. By examining the eigenvalues of the Jacobian, one can determine whether the equilibrium is stable or unstable. The stability of a system described by nonlinear differential equations is often studied using the Jacobian matrix to linearize the system around equilibrium points. We now calculate the Jacobian matrix at E

$$J_E = \begin{bmatrix} -\alpha_1 + \alpha_1\xi - \alpha_1(a + 3bw^2) & \alpha_1 & 0 & -6\alpha_1 bwx \\ 1 & -1 & 1 & 0 \\ 0 & -\beta_1 & -\gamma & 0 \\ 1 & 0 & 0 & 0 \end{bmatrix}. \tag{11}$$

Then, the characteristic equation is obtained as

$$\lambda^4 + c_1\lambda^3 + c_2\lambda^2 + c_3\lambda = 0, \tag{12}$$

where

$$\begin{aligned} c_1 &= (1 + \gamma + \alpha_1 - \alpha_1\xi + \alpha_1(a + 3bw^2)), \\ c_2 &= (\beta_1 + (1 + \alpha_1)\gamma - \alpha_1\xi(1 + \gamma) + \alpha_1(a + 3bw^2)(1 \\ &\quad + \gamma)), \\ c_3 &= \alpha_1(\beta_1 + (a + 3bw^2 - \xi)(\beta_1 + \gamma)). \end{aligned} \tag{13}$$

We shall write Hurwitz matrix which is given by

$$H = \begin{bmatrix} c_1 & c_3 & 0 \\ 1 & c_2 & 0 \\ 0 & c_1 & c_3 \end{bmatrix}. \tag{14}$$

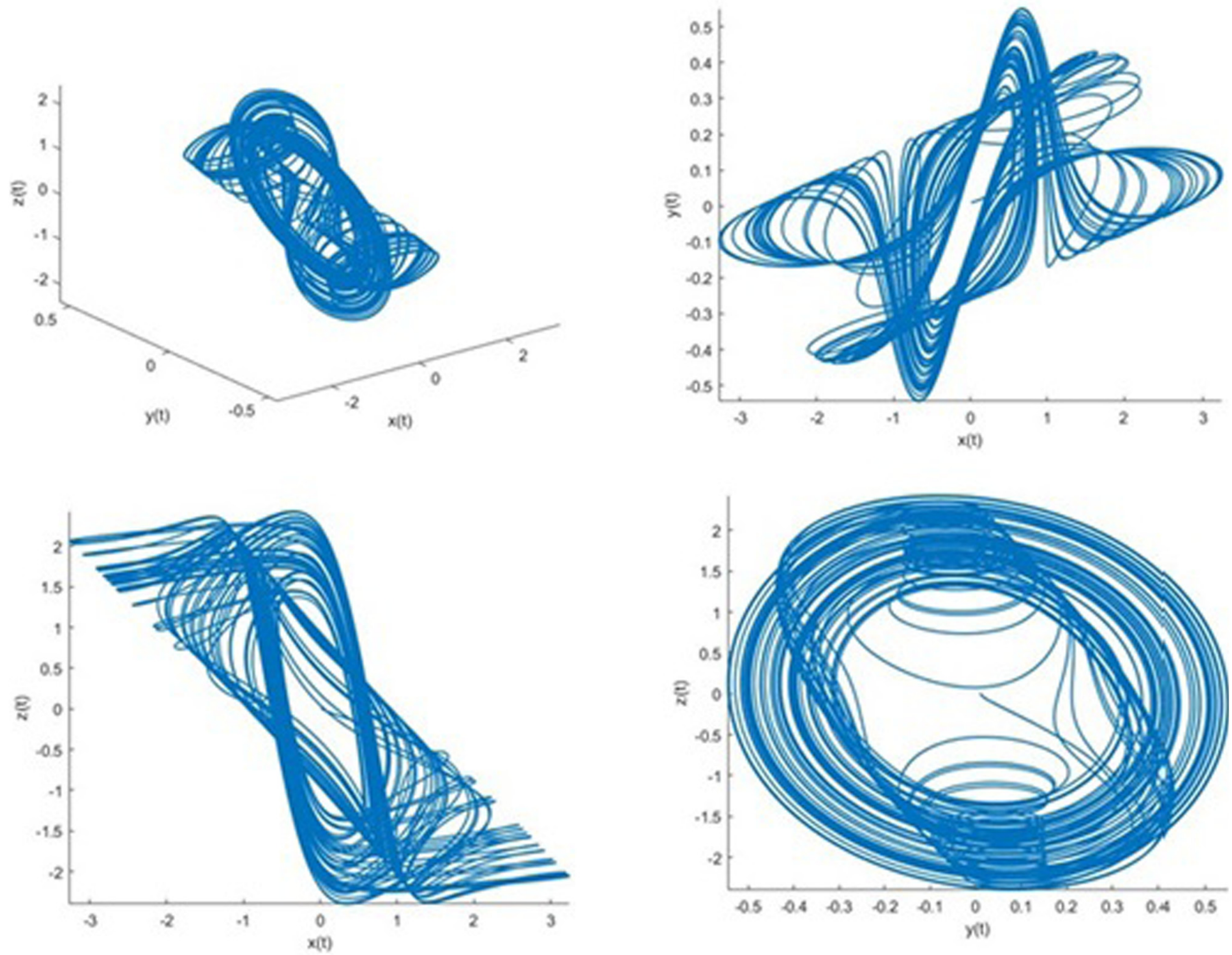

Figure 1: The graphical representation of the memristor system with initial conditions $x(0) = y(0) = z(0) = w(0) = 0.001$.

According to the Routh–Hurwitz condition, all eigenvalues have negative real parts except for one, which has a value of zero under the conditions:

$$\begin{aligned} &H_1 : c_1 > 0, \\ &H_2 : c_1 c_2 - c_3 > 0, \\ &H_3 : c_3(c_1 c_2 - c_3) > 0. \end{aligned} \tag{15}$$

2.1.2 Dissipativity of system

A dissipative system is defined by the formation of complex structures, sometimes chaotic, in which interacting particles display long-range correlations. The dissipativity of system is formulated by

$$\begin{aligned} \nabla D &= \frac{\partial \dot{x}}{\partial x} + \frac{\partial \dot{y}}{\partial y} + \frac{\partial \dot{z}}{\partial z} + \frac{\partial \dot{w}}{\partial w} \\ &= -\alpha_1(a+1) + \alpha_1 \xi - \alpha_1 3bw^2 - \gamma. \end{aligned} \tag{16}$$

We conclude that when $\alpha_1 \xi < \alpha_1(a+1) + 3\alpha_1 bw^2 + \gamma$, the considered system is dissipative, meaning that its asymptotic motion converges toward an attractor and each volume surrounding the system's trajectory decreases exponentially as $t \to \infty$.

$$\frac{\mathrm{d}D}{\mathrm{d}t} = e^{-\alpha_1(a+1)+\alpha_1\xi-\alpha_1 3bw^2-\gamma}. \tag{17}$$

Consequently, the attractor's volume decreases by a factor of $-\alpha_1(a+1) + \alpha_1\xi - \alpha_1 3bw^2 - \gamma$.

2.1.3 Lyapunov exponents

A qualitative representation of the dynamics of a system is provided by the sign of the Lyapunov exponent. One-dimensional maps have a single Lyapunov exponent that is positive for chaos, zero for a marginally stable trajectory and negative for a periodic trajectory. In a continuous dissipative dynamical system with three dimensions, the spectra and attractors that can be described are characterized under the following conditions:

- The chaotic system is a strange attractor if $\lambda_1 > 0, \lambda_2 = 0, \lambda_3 < 0$.
- The chaotic system is a torus if $\lambda_1 = 0, \lambda_2 = 0, \lambda_3 < 0$.
- The chaotic system is a limit cycle if $\lambda_1 < 0, \lambda_2 = 0, \lambda_3 < 0$.
- The chaotic system is a fixed point if $\lambda_1 < 0, \lambda_2 < 0, \lambda_3 < 0$.

We intend to calculate Lyapunov exponents with the help of Wolf's algorithm [19]. The Lyapunov exponents are evaluated as follows:

$$L_1 = 3.1948, \quad L_2 = 0.9884, \quad L_3 = 0, \quad L_4 = -6.0166, \tag{18}$$

and the Lyapunov dimension is

$$D_L = n + \frac{1}{|L_{n+1}|}\sum_{k=1}^{n} L_k = 3 + \frac{0.9884 + 3.1948}{6.0166} = 3.695. \tag{19}$$

In light of the phase portraits, Lyapunov exponents, and Lyapunov dimension, it is evident that the fourth-order memristive circuit is exhibiting chaotic behavior. The Lyapunov exponents for the considered model are depicted in Figure 2.

2.2 Existence and uniqueness of the memristor model with fractal–fractional derivative with Mittag–Leffler kernel

This section delves into analyzing the existence and uniqueness of the memristor model with a fractal–fractional derivative with Mittag–Leffler kernel by employing the Banach's fixed-point and Krasnoselskii's fixed-point theorem [18,20–23]. Before proceeding with the analysis, we consider a Banach space on $\Lambda \coloneqq [0, T]$ of all continuous real-valued functions denoted as $X = C(\Lambda \times \mathbb{R}^4, \mathbb{R})$ equipped with the norm

$$\begin{aligned} \|Y\| &= \|(x, y, z, w)\| \\ &= \|x\| + \|y\| + \|z\| + \|w\|, \end{aligned} \tag{20}$$

and

$$\|Y_i\| = \sup_{t\in\Lambda}|Y_i(t)|, \; Y_i \in X. \tag{21}$$

In order to avoid intricacy, we also define the following notations:

$$\begin{aligned} Y(t) &= \begin{bmatrix} Y_1(t) \\ Y_2(t) \\ Y_3(t) \\ Y_4(t) \end{bmatrix} = \begin{bmatrix} x(t) \\ y(t) \\ z(t) \\ w(t) \end{bmatrix}, \\ G(t, Y(t)) &= \begin{bmatrix} G_1(t, Y(t)) \\ G_2(t, Y(t)) \\ G_3(t, Y(t)) \\ G_4(t, Y(t)) \end{bmatrix} = \begin{bmatrix} \alpha_1(y - x + \xi x - W(w)x) \\ x - y + z \\ -\beta_1 y - \gamma z \\ x \end{bmatrix}. \end{aligned} \tag{22}$$

Lemma 2.1. *Let $G \in X$ and $Y \in C(\Lambda, \mathbb{R})$, then the memristor model with fractal–fractional derivative with Mittag–Leffler kernel can be written as*

$$\begin{aligned} {}^{\mathrm{FFM}}_{t_0}D_t^{\alpha,\beta} Y(t) &= G(t, Y(t)), \quad \text{if } t > t_0 \\ Y(0) &= Y_0, \quad \text{if } t = t_0. \end{aligned} \tag{23}$$

The integral equation that corresponds to the above equation is derived by applying the associated integral as follows:

$$\begin{aligned} Y(t) &= \beta t^{\beta-1}(1-\alpha)G(t, Y(t)) \\ &\quad + \frac{\alpha\beta}{\Gamma(\alpha)}\int_0^t s^{\beta-1}(t-s)^{\alpha-1}G(s, Y(s))\mathrm{d}s. \end{aligned} \tag{24}$$

We shall define an operator $T : X \to X$ such that

$$\begin{aligned} (T_1 Y)(t) &= \beta t^{\beta-1}(1-\alpha)G(t, Y(t)) \\ &\quad + \frac{\alpha\beta}{\Gamma(\alpha)}\int_0^t s^{\beta-1}(t-s)^{\alpha-1}G(s, Y(s))\mathrm{d}s. \end{aligned} \tag{25}$$

In order to explore the fixed point theory, we convert the given model into the fixed point problem ($Y = TY$). Our following step involves proving the existence of a unique solution for the memristor model incorporating a fractal–fractional derivative with a Mittag–Leffler kernel.

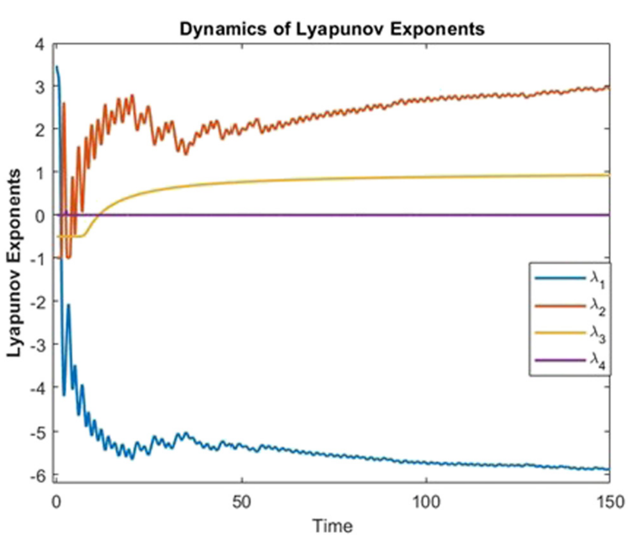

Figure 2: The visualization of the dynamics of the Lyapunov exponents.

Theorem 2.1. *Suppose that $G \in X$ satisfies the following condition*:

(A_1) *There exists a constant $L_{\max} > 0$, where $L_{\max} = \max\{L_1, L_2, L_3, L_4\}$, such that*

$$|G(t, Y(t)) - G(t, Y^*(t))| \leqslant L_{\max}\left(\sum_{i=1}^{4}|Y_i(t) - Y_i^*(t)|\right) \quad (26)$$

for any $Y_i \in X$ and $t \in \Lambda$. If

$$\left(\beta(1-\alpha)T_{\min}^{\beta-1} + \frac{\alpha\beta T^{\alpha+\beta-1}}{\Gamma(\alpha)}B(\beta,\alpha)\right)L_{\max} < 1, \quad (27)$$

then the memristor model with fractal–fractional derivative with Mittag–Leffler kernel has a unique solution.

Proof. Now, let D_{r_1} be a bounded, closed, and convex subset such that

$$D_{r_1} = \{(x, y, z, w) \in X : \|(x, y, z, w)\| \leq r_1\}$$

with a radius

$$r_1 \geqslant \frac{P_{\max} + \beta(1-\alpha)T_{\min}^{\beta-1} + \frac{\alpha T^{\alpha+\beta-1}}{\Gamma(\alpha)}B(\beta,\alpha)G_{\max}^*}{1 - \beta(1-\alpha)T_{\min}^{\beta-1} + \frac{\alpha\beta T^{\alpha+\beta-1}}{\beta\Gamma(\alpha)}B(\beta,\alpha)L_{\max}}, \quad (28)$$

where $P_{\max} = \max\{Y_{i_0}\}$, $G_{\max}^* = \{G_i^*\}$ and let $\sup_{t\in\Lambda}|G_i(t, 0)| = G_i^* < \infty$ for $i = 1,\ldots, 4$.

Step 1. We shall show $TD_{r_1} \subset D_{r_1}$. For any $Y_i \in D_{r_1}$, $t \in T$, we write the following inequality:

$$\begin{aligned}|(T_iY_i)(t)| &\leq \beta t^{\beta-1}(1-\alpha)|G_i(t, Y_i(t))| \\ &\quad + \frac{\alpha\beta}{\Gamma(\alpha)}\int_0^t s^{\beta-1}(t-s)^{\alpha-1}|G_i(s, Y_i(s))|\mathrm{d}s \\ &\leq \beta t^{\beta-1}(1-\alpha)[|G_i(t, Y_i(t)) - G_i(t, 0)| + |G_i(t, 0)|] \\ &\quad + \frac{\alpha\beta}{\Gamma(\alpha)}\int_0^t s^{\beta-1}(t-s)^{\alpha-1}[|G_i(s, Y_i(s)) \\ &\quad - G_1(s, 0)| + |G_1(s, 0)|]\mathrm{d}s \\ &\leq \beta t^{\beta-1}(1-\alpha)\left[L_i\left(\sum_{i=1}^{4}|Y_i(t)|\right) + G_i^*\right] \\ &\quad + \frac{\alpha\beta}{\Gamma(\alpha)}\int_0^t s^{\beta-1}(t-s)^{\alpha-1}\left[L_i\left(\sum_{j=1}^{4}|Y_j(s)|\right) + G_i^*\right]\mathrm{d}s \\ &\leq \left(\beta(1-\alpha)T_{\min}^{\beta-1} + \frac{\alpha\beta}{\Gamma(\alpha)}T^{\alpha+\beta-1}B(\beta,\alpha)\right) \\ &\quad \times \left[L_i\left(\sum_{j=1}^{4}\|Y_j\|\right) + G_i^*\right],\end{aligned} \quad (29)$$

which leads to

$$\|(T_iY_i)(t)\| \leq \left(\beta(1-\alpha)T_{\min}^{\beta-1} + \frac{\alpha\beta}{\Gamma(\alpha)}T^{\alpha+\beta-1}B(\beta,\alpha)\right)[L_ir_1 + G_i^*], \quad (30)$$

where $B(\beta, \alpha)$ is the Beta function. From the above inequality, we conclude that $TD_{r_1} \subset D_{r_1}$.

Step II. We shall show that T is a contraction. Assuming that $Y_h \in D_{r_1}$, $Y_h^* \in D_{r_1}$, then we have

$$\begin{aligned}&|(T_iY_i)(t) - (T_iY_i^*)(t)| \\ &\leq \beta t^{\beta-1}(1-\alpha)|G_i(t, Y_i(t)) - G_i(t, Y_i^*)(t)| \\ &\quad + \frac{\alpha\beta}{\Gamma(\alpha)}\int_0^t s^{\beta-1}(t-s)^{\alpha-1}|G_i(s, Y_i(s)) \\ &\quad - G_1(s, Y_i^*(s))|\mathrm{d}s \leq \beta t^{\beta-1}(1-\alpha)L_i\left(\sum_{j=1}^{4}|Y_j(t) \right. \\ &\quad \left. - Y_j^*(t)|\right) + \frac{\alpha\beta}{\Gamma(\alpha)}\int_0^t s^{\beta-1}(t-s)^{\alpha-1} \\ &\quad \times \left[L_i\left(\sum_{j=1}^{4}|Y_j(s) - Y_j^*(s)|\right)\right]\mathrm{d}s \leq \left(\beta(1-\alpha)T_{\min}^{\beta-1}\right. \\ &\quad \left. + \frac{\alpha\beta}{\Gamma(\alpha)}T^{\alpha+\beta-1}B(\beta,\alpha)\right) \times L_i\left(\sum_{j=1}^{4}\|Y_j - Y_j^*\|\right).\end{aligned} \quad (31)$$

We arrange (31) as follows:

$$\begin{aligned}&|(T_iY_i)(t) - (T_iY_i^*)(t)| \\ &\leq \left(\beta(1-\alpha)T_{\min}^{\beta-1} + \frac{\alpha\beta}{\Gamma(\alpha)}T^{\alpha+\beta-1}B(\beta,\alpha)\right)L_i \\ &\quad \times \left(\sum_{j=1}^{4}\|Y_j - Y_j^*\|\right).\end{aligned} \quad (32)$$

Since $T = (T_1, T_2, \ldots)$ and $L_{\max} > 0$ with the above inequality, we obtain

$$\begin{aligned}&\|TY_i - TY_i^*\| \\ &\leq \left(\beta(1-\alpha)T_{\min}^{\beta-1} + \frac{\alpha\beta}{\Gamma(\alpha)}T^{\alpha+\beta-1}B(\beta,\alpha)\right)L_{\max} \\ &\quad \times \left(\sum_{j=1}^{4}\|Y_j - Y_j^*\|\right).\end{aligned} \quad (33)$$

By the condition $\left(\beta(1-\alpha)T_{\min}^{\beta-1} + \frac{\alpha\beta}{\Gamma(\alpha)}T^{\alpha+\beta-1}B(\beta,\alpha)\right)$, $L_{\max} < 1$, then we can conclude that T is a contraction. Therefore, by Lemma 1.1, the memristor model with the fractal–fractional derivative model has a solution. □

Theorem 2.2. *In addition to the assumption that $G \in X$ satisfies the assumptions (A_1) in* Theorem 2.1, *we also present the following condition*:

(A_2) *There exist constants $g_{ij} > 0$, $i = 0,\ldots 4$, $j = 1,\ldots, 4$ such that*

$$|G(t, Y_i(t))| \leq g_{0j} + \sum_{i=1}^{4} + g_{ij}|Y_i(t)|. \tag{34}$$

If

$$\beta(1-\alpha)T_{\min}^{\beta-1}L_{\max} < 1, \tag{35}$$

then the memristor model with fractal–fractional model has at least one solution.

Proof. We define a set $D_{r_2} \coloneqq \{(Y_h) \in X : \|Y_h\| \leq r_2\}$. We first define two operators $Q, P : D_{r_2} \to X$ such that $Q = (Q_1, Q_2, Q_3, Q_4)$ and $P = (P_1, P_2, P_3, P_4)$. The operator Q is defined by

$$(Q_iY_i)(t) = \beta t^{\beta-1}(1-\alpha)G_i(t, Y_i(t)), \tag{36}$$

and the operator P is defined as

$$(P_iY_i)(t) = \frac{\alpha\beta}{\Gamma(\alpha)}\int_0^t s^{\beta-1}(t-s)^{\alpha-1}G_i(s, Y_i(s))\mathrm{d}s. \tag{37}$$

Using (A_1) in Theorem 2.1, for any $Y \in D_{r_1}$, and $Y^* \in D_{r_1}$, we have

$$\begin{aligned}\|Q_iY_i - Q_iY_i^*\| &\leq \beta(1-\alpha)T_{\min}^{\beta-1}\sup_{t\in\Lambda} \\ &\quad\times |G_i(t, Y_i(t)) - G_i(t, Y_i^*(t))| \\ &\leq \beta(1-\alpha)T_{\min}^{\beta-1}L_i\left(\sum_{j=1}^{4}\|Y_j - Y_j^*\|\right).\end{aligned} \tag{38}$$

Considering the above inequality with $L_{\max}$, it follows that

$$\|QY - QY^*\| \leq \beta(1-\alpha)T_{\min}^{\beta-1}L_{\max}\|Y - Y^*\|. \tag{39}$$

Therefore, it follows that Q is a contraction.

Our subsequent step involves proving the continuous and compact nature of P, resulting in the establishment of complete continuity of P. This then becomes a sufficient condition for demonstrating the boundedness and equicontinuity of P. The continuity of P is clearly evident when considering (A_2) and the continuity of Q. To show the boundness of P, we have the following for any $t \in \Lambda$:

$$\begin{aligned}\|P_iY_i\| &\leq \frac{\alpha\beta}{\Gamma(\alpha)}\sup\left|\int_0^t s^{\beta-1}(t-s)^{\alpha-1}|G_i(s, Y_i(s))|\mathrm{d}s\right| \\ &\leq \frac{\alpha\beta}{\Gamma(\alpha)}\int_0^t s^{\beta-1}(t-s)^{\alpha-1}\sup_{t\in\Lambda}|G_i(s, Y_i(s))|\mathrm{d}s \\ &\leq \frac{\alpha\beta}{\Gamma(\alpha)}T^{\alpha+\beta-1}B(\beta,\alpha)\left[g_{0i} + \sum_{j=1}^{4}g_{ji}|Y_i(t)|\right].\end{aligned} \tag{40}$$

By applying the above inequality and setting $\|P\| = \max\{\|P_i\|\}_{i=1,\ldots,4}$ with $g_j^* = \max\{g_{ji}\}_{i=1,\ldots,4}$, it follows that

$$\|P(x,y,z,w)\| \leq \frac{\alpha\beta}{\Gamma(\alpha)}T^{\alpha+\beta-1}B(\beta,\alpha)\left[g_0^* + \sum_{j=1}^{4}g_j^*\|Y_i\|\right]. \tag{41}$$

Then, it is concluded that P is bounded. Next we shall show that P is equicontinuity. Suppose that $t_1, t_2 \in \Lambda$ with $0 \leq t_1 \leq t_2 \leq \Lambda$, we obtain

$$\begin{aligned}&|(P_iY_i)(t_2) - (P_iY_i)(t_1)| \\ &\leq \frac{\alpha\beta}{\Gamma(\alpha)}\left|\begin{matrix}\int_0^{t_2} s^{\beta-1}(t_2-s)^{\alpha-1}|G_i(s, Y_i(s))|\mathrm{d}s \\ -\int_0^{t_1} s^{\beta-1}(t_1-s)^{\alpha-1}|G_i(s, Y_i(s))|\mathrm{d}s\end{matrix}\right| \\ &\leq \frac{\alpha\beta}{\Gamma(\alpha)}B(\beta,\alpha)\left[g_{0i} + r_2\sum_{j=1}^{4}g_{ji}\right] \\ &\quad\times |t_1^{\alpha+\beta-1} - t_2^{\alpha+\beta-1} + 2(t_2-t_1)^{\alpha+\beta-1}|.\end{aligned} \tag{42}$$

It is important to note that the right side of the inequality is independent of Y_i and $|(P_iY_i)(t_2) - (P_iY_i)(t_1)| \to 0$ as $t_2 \to t_1$, it indicates that P_i is bounded, uniformly continuous, and compact that P_i is completely continuous. By using the above inequality and taking the norm of P, we can have

$$\begin{aligned}&|(PY)(t_2) - (PY)(t_1)| \\ &\leq \frac{\alpha\beta}{\Gamma(\alpha)}B(\beta,\alpha)\left[g_0^* + r_2\sum_{j=1}^{4}g_j^*\right] \\ &\quad\times |t_1^{\alpha+\beta-1} - t_2^{\alpha+\beta-1} + 2(t_2-t_1)^{\alpha+\beta-1}|.\end{aligned} \tag{43}$$

Then, P is bounded, uniformly continuous, and compact that P is completely continuous. Therefore, by Lemma 2.2, memristor model with fractal–fractional derivative with Mittag–Leffler kernel has at least one solution. □

3 Memristor model with piecewise memductance function

The objective of this section is to analyze the results of the modified model, such as memory effects, long- and chaotic tendencies, when the piecewise memductance function is added to the memristor system [4] and also replaces the classical derivative with fractal–fractional derivatives. The memristor system with piecewise memductance function is depicted by

$$\begin{cases} \dot{x}(t) = \alpha_1(y - x + \xi x - W(w)x), \\ \dot{y}(t) = x - y + z, \\ \dot{z}(t) = -\beta_1 y - \gamma z, \\ \dot{w}(t) = x, \end{cases} \tag{44}$$

where $W(w)$ is the memductance function. A cubic piecewise function is proposed as follows:

$$\begin{aligned} W(w) &= \frac{\mathrm{d}q}{\mathrm{d}w} \\ &= \frac{\mathrm{d}}{\mathrm{d}w}\begin{cases} (aw + bw^3), & \text{if } 0 \le t \le t_0 \\ \frac{1}{2}a_1 w^2\left(c_1 + \frac{2}{3}b_1 w\right), & \text{if } t_0 \le t \le T. \end{cases} \\ &= \begin{cases} (a + 3bw^2), & \text{if } 0 \le t \le t_0 \\ a_1 w(c_1 + b_1 w), & \text{if } t_0 \le t \le T. \end{cases} \end{aligned} \tag{45}$$

To observe the numerical simulations, we shall obtain the numerical solution of the memristor model by employing the Adams–Bashforth method

$$\begin{cases} \dot{x}(t) = \alpha_1(y - x + \xi x - W(w)x), \\ \dot{y}(t) = x - y + z, \\ \dot{z}(t) = -\beta_1 y - \gamma z, \\ \dot{w}(t) = x. \end{cases} \tag{46}$$
$$x(0) = x_0, y(0) = y_0, z(0) = z_0, w(0) = w_0.$$

Applying the integral on both sides and taking the difference of the equations written at $t = t_k$ and $t = t_{k+1}$, we obtain the following:

$$\begin{aligned} x(t_{k+1}) &= x(t_k) + \int_{t_k}^{t_{k+1}} (\alpha_1(y - x + \xi x - W(w)x))\mathrm{d}s, \\ y(t_{k+1}) &= y(t_k) + \int_{t_k}^{t_{k+1}} (x - y + z)\mathrm{d}s, \\ z(t_{k+1}) &= z(t_k) + \int_{t_k}^{t_{k+1}} (-\beta_1 y - \gamma z)\mathrm{d}s, \\ w(t_{k+1}) &= w(t_k) + \int_{t_k}^{t_{k+1}} x\mathrm{d}s. \end{aligned} \tag{47}$$

When approximating the functions on the right hand side of the above equations with Lagrange polynomials [24], we obtain the following numerical scheme for memristor system:

$$\begin{aligned} x^{k+1} &= x^k + \frac{3h}{2}\alpha_1(y^k - x^k + \xi x^k - W(w^k)x^k) \\ &\quad - \frac{h}{2}\alpha_1(y^{k-1} - x^{k-1} + \xi x^{k-1} - W(w^{k-1})x^{k-1}), \\ y^{k+1} &= y^k + \frac{3h}{2}(x^k - y^k + z^k) - \frac{h}{2}(x^{k-1} - y^{k-1} \\ &\quad + z^{k-1}), \\ z^{k+1} &= z^k + \frac{3h}{2}(-\beta_1 y^k - \gamma z^k) - \frac{h}{2}(-\beta_1 y^{k-1} - \gamma z^{k-1}), \\ w^{k+1} &= w^k + \frac{3h}{2}x^k - \frac{h}{2}x^{k-1}. \end{aligned} \tag{48}$$

During the simulations, the initial condition and parameters are chosen as

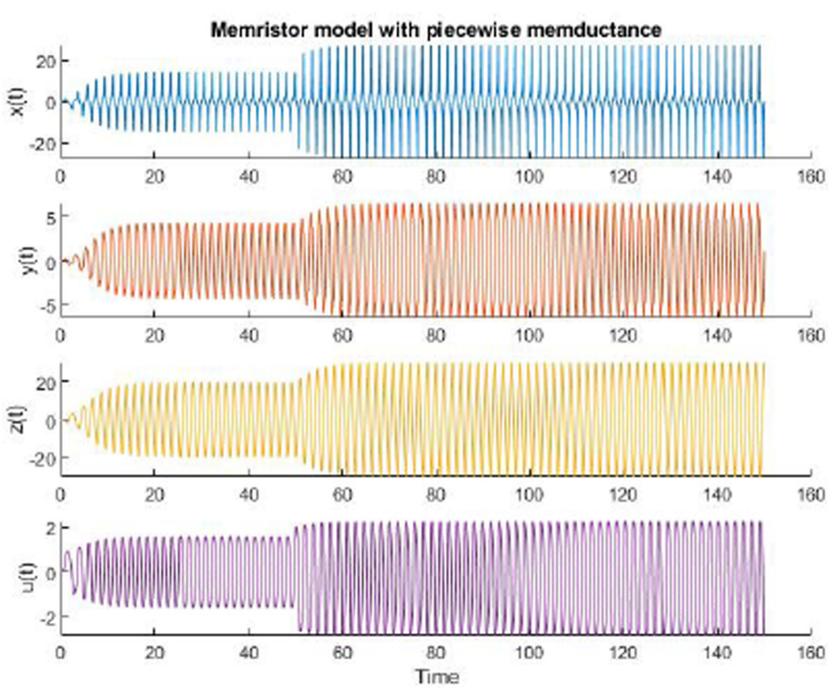

Figure 3: The graphical representation of the classical memristor system with piecewise memductance.

$$
\begin{gathered}
x(0) = 0.001, \quad y(0) = 0.001, \\
z(0) = 0.001, \quad w(0) = 0.001, \\
\alpha_1 = 16.4, \quad \xi = 1.4, \quad \beta_1 = 15, \quad \gamma = 0.5, \\
a = 0.2, \quad b = 0.4, \\
a_1 = 2.32, \quad b_1 = 0.24, \quad c_1 = 0.4.
\end{gathered} \tag{49}
$$

The numerical simulation for each class of the model with classical derivative is depicted in Figure 3.

The numerical simulation for memristor model in 3D perspective is shown in Figure 4.

3.1 Numerical solution of memristor model with fractal–fractional derivative with exponential kernel

In this subsection, we present the numerical solution of the memristor model with fractal–fractional derivative with exponential kernel [13]

$$
\begin{cases}
{}_{t_0}^{t}D_{\alpha,\beta}X_i(t) = F(X_i, t), & \text{if } t > t_0 \\
X_i(t_0) = X_{i,0}, & \text{if } t = t_0.
\end{cases} \tag{50}
$$

Here we denote for simplicity

$$
X_i(t) = \begin{bmatrix} x(t) \\ y(t) \\ z(t) \\ w(t) \end{bmatrix}, \quad
F(X_i, t) = \begin{bmatrix} f_1(X_i, t) \\ f_2(X_i, t) \\ f_3(X_i, t) \\ f_4(X_i, t) \end{bmatrix}, \tag{51}
$$

where $i = 1, \ldots, 4$. Applying the associated integral, we obtain

$$
X(t) = (1-\alpha)\beta t^{\beta-1} F_i(t, X_i(t)) + \alpha\beta \int_{t_0}^{t} s^{\beta-1} F_i(s, X_i(s))\mathrm{d}s. \tag{52}
$$

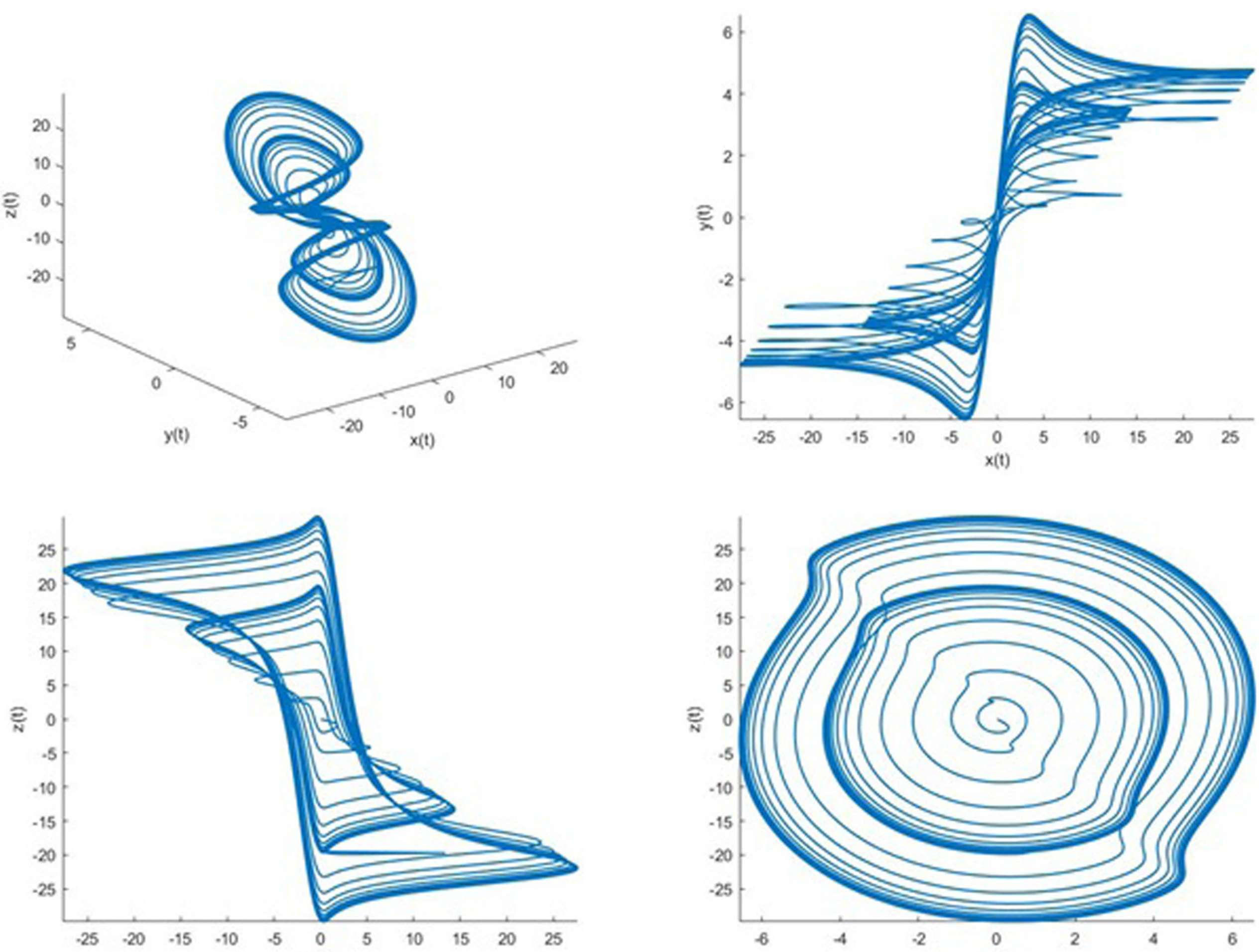

Figure 4: The 3D graphical representation of the classical memristor system with piecewise memductance.

We obtain the following scheme by the approximation of the function $F_i(t, X_i(t))$ using the Lagrange polynomial at $t = t_k$ and $t = t_{k+1}$

$$\begin{aligned} X_i^{k+1} = X_i^k &+ (1-\alpha)\beta t_k^{\beta-1} \\ &\times [F_i(t_k, X_i^k) - F_i(t_{k-1}, X_i^{k-1}(t))] \\ &+ \frac{3\alpha\beta h}{2} t_k^{\beta-1} F_i(t_k, X_i^k(t)) \\ &- \frac{\alpha\beta h}{2} t_{k-1}^{\beta-1} F_i(t_{k-1}, X_i^{k-1}(t)). \end{aligned} \tag{53}$$

We consider our system with fractal–fractional derivative with exponential kernel

$$\begin{cases} {}_{t_0}^{t}D_{\alpha,\beta} x(t) = \alpha_1(y - x + \xi x - W(w)x) \\ {}_{t_0}^{t}D_{\alpha,\beta} y(t) = x - y + z \\ {}_{t_0}^{t}D_{\alpha,\beta} z(t) = (-\beta_1 y - \gamma z) \\ {}_{t_0}^{t}D_{\alpha,\beta} w(t) = x. \end{cases} \tag{54}$$

The estimation of the parameters of the model and initial data is considered as

$$\begin{aligned} &x(0) = 0.001, \quad y(0) = 0.001, \\ &z(0) = 0.001, \quad w(0) = 0.001, \\ &\alpha_1 = 13.4, \quad \xi = 1.4, \quad \beta_1 = 11, \\ &\gamma = 0.2, \quad a = 0.2, \quad b = 0.4, \\ &a_1 = 2.32, \quad b_1 = 0.24, \quad c_1 = 0.14. \end{aligned} \tag{55}$$

The numerical simulation for the model in the case of fractal–fractional derivative with exponential kernel is shown in Figure 5.

3.2 Numerical solution of memristor model with fractal–fractional derivative with power-law

For fractal–fractional derivative with power-law case [13], we consider the following memristor model:

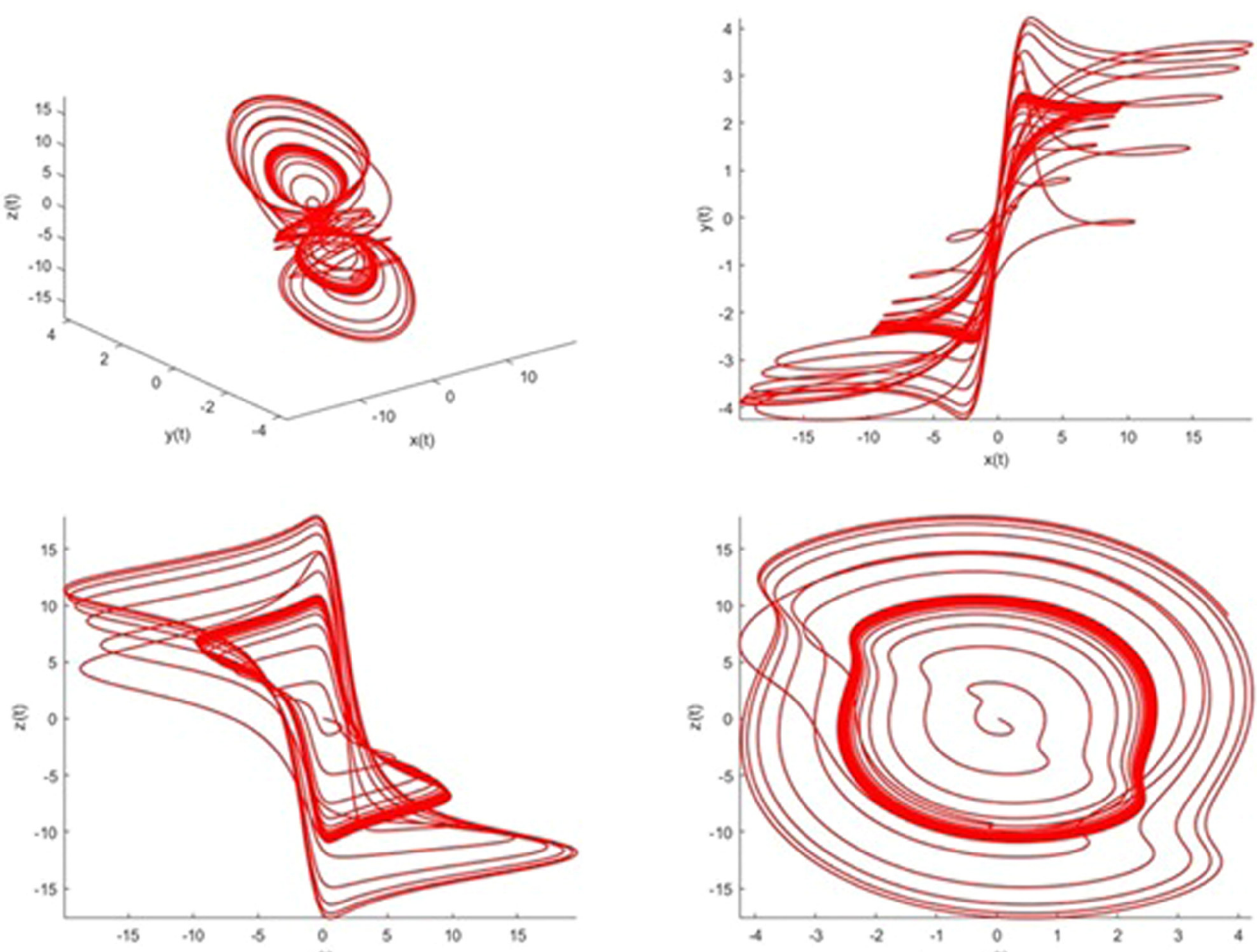

Figure 5: The graphical representation of the chaotic behavior of the fractal–fractional memristor system with piecewise memductance for $\alpha = 0.99$ and $\beta = 0.99$.

$$\begin{cases} {}^{\mathrm{FFP}}_{t_0}D^{\alpha,\beta}_{t}X_i(t) = F(X_i, t), & \text{if } t > t_0 \\ X_i(t_0) = X_{i,0}, & \text{if } t = t_0. \end{cases} \tag{56}$$

Applying the associated integral, we obtain

$$X_i(t) = \frac{\beta}{\Gamma(\alpha)}\int_{t_0}^{t} s^{\beta-1}F_i(s, X_i(s))(t-s)^{\alpha-1}\mathrm{d}s. \tag{57}$$

We obtain the following:

$$X_i(t_{k+1}) = \frac{\beta}{\Gamma(\alpha)}\int_{0}^{t_{k+1}} s^{\beta-1}F_i \times (s, X_i(s))(t_{k+1}-s)^{\alpha-1}\mathrm{d}s. \tag{58}$$

Replacing Lagrange polynomials of the functions $F_i(t, X_i(t))$ in the above equation [24], we obtain the following:

$$X_i^{k+1} = \begin{cases} \frac{\beta}{\Gamma(\alpha)}\sum_{m=0}^{k}\frac{t_m^{\beta-1}F_i(t_m, X_i^m)}{h} \\ \int_{t_m}^{t_{m+1}}(s-t_{k-1})(t_{k+1}-s)^{\alpha-1}\mathrm{d}s \\ -\frac{\beta}{\Gamma(\alpha)}\sum_{m=0}^{k} t_{m-1}^{\beta-1}F_i(t_{m-1}, X_i^{m-1}) \\ \int_{t_m}^{t_{m+1}}(s-t_k)(t_{k+1}-s)^{\alpha-1}\mathrm{d}s. \end{cases} \tag{59}$$

Then, the numerical scheme for memristor system with piecewise memductance is represented by the following:

$$X_i^{k+1} = \begin{cases} \frac{\beta h^\alpha}{\Gamma(\alpha+2)}\sum_{m=0}^{k} t_m^{\beta-1}F_i(t_m, X_i^m) \\ \begin{bmatrix}(k-m+1)^\alpha(k-m+2+\alpha) \\ -(k-m)^\alpha(k-m+2+2\alpha)\end{bmatrix} \\ -\frac{\beta h^\alpha}{\Gamma(\alpha+2)}\sum_{m=0}^{k} t_{m-1}^{\beta-1}F_i(t_{m-1}, X_i^{m-1}) \\ \begin{bmatrix}(k-m+1)^{\alpha+1} \\ -(k-m)^\alpha(k-m+1+\alpha)\end{bmatrix}. \end{cases} \tag{60}$$

We consider our system with fractal–fractional derivative with fractal–fractional derivative with power-law

$$\begin{cases} {}^{\mathrm{FFP}}_{t_0}D^{\alpha,\beta}_{t}x(t) = \alpha_1(y - x + \xi x - W(w)x), \\ {}^{\mathrm{FFP}}_{t_0}D^{\alpha,\beta}_{t}y(t) = x - y + z, \\ {}^{\mathrm{FFP}}_{t_0}D^{\alpha,\beta}_{t}z(t) = (-\beta_1 y - \gamma z), \\ {}^{\mathrm{FFP}}_{t_0}D^{\alpha,\beta}_{t}w(t) = x. \end{cases} \tag{61}$$

The estimation of the parameters of the model and initial data is considered as

$$\begin{gathered} x(0) = 0.001 \quad y(0) = 0.001, \\ z(0) = 0.001 \quad w(0) = 0.001, \\ \alpha_1 = 13.4, \quad \xi = 1.4, \quad \beta_1 = 15, \\ \gamma = 0.2, \quad a = 0.2, \quad b = 0.4, \\ a_1 = 2.32, \quad b_1 = 0.24, \quad c_1 = 0.14. \end{gathered} \tag{62}$$

The numerical simulation for the memristor model in the case of fractal–fractional derivative with power-law is shown in Figure 6.

3.3 Numerical solution of memristor model with fractal–fractional derivative with Mittag–Leffler kernel

We consider the memristor system with fractal–fractional derivative with Mittag–Leffler kernel [13]

$$\begin{cases} {}^{\mathrm{FFM}}_{t_0}D^{\alpha,\beta}_{t}X_i(t) = F(X_i, t), & \text{if } t > t_0 \\ X_i(t_0) = X_{i,0}, & \text{if } t = t_0. \end{cases} \tag{63}$$

Applying the associated integral, we obtain

$$X_i(t) = (1-\alpha)\beta t^{\beta-1}F_i(t, X_i) + \frac{\alpha\beta}{\Gamma(\alpha)}\int_{t_0}^{t} s^{\beta-1}F_i(s, X_i(s))(t-s)^{\alpha-1}\mathrm{d}s. \tag{64}$$

We obtain the following:

$$X_i(t_{k+1}) = (1-\alpha)\beta t^{\beta-1}F_i(t, X_i) + \frac{\alpha\beta}{\Gamma(\alpha)}\int_{0}^{t_{k+1}} s^{\beta-1}F_i(s, X_i(s))(t_{k+1}-s)^{\alpha-1}\mathrm{d}s. \tag{65}$$

Replacing Lagrange polynomials of the functions $F_i(s, X_i(s))$ in the above equation [24], we obtain the following:

$$X_i^{k+1} = \begin{cases} (1-\alpha)(\beta t_k^{\beta-1}F_i(t_k, X_i^k)) \\ +\frac{\alpha\beta}{\Gamma(\alpha)}\sum_{m=0}^{k} t_m^{\beta-1}\frac{F_i(t_m, X_i^m)}{h} \\ \int_{t_m}^{t_{m+1}}(s-t_{k-1})(t_{k+1}-s)^{\alpha-1}\mathrm{d}s \\ -\frac{\alpha\beta}{\Gamma(\alpha)}\sum_{m=0}^{k} t_{m-1}^{\beta-1}\frac{F_i(t_{m-1}, X_i^{m-1})}{h} \\ \int_{t_m}^{t_{m+1}}(s-t_k)(t_{k+1}-s)^{\alpha-1}\mathrm{d}s. \end{cases} \tag{66}$$

Then, the numerical scheme for memristor system with piecewise memductance is represented by the following:

$$X_i^{k+1} = \begin{cases} (1-\alpha)(\beta t_k^{\beta-1} F_i(t_k, X_i^k)) \\ + \dfrac{\alpha\beta h^\alpha}{\Gamma(\alpha+2)} \displaystyle\sum_{m=0}^{k} t_m^{\beta-1} F_i(t_m, X_i^m) \\ \begin{bmatrix} (k-m+1)^\alpha (k-m+2+\alpha) \\ -(k-m)^\alpha (k-m+2+2\alpha) \end{bmatrix} \\ - \dfrac{\alpha\beta h^\alpha}{\Gamma(\alpha+2)} \displaystyle\sum_{m=0}^{k} t_{m-1}^{\beta-1} F_i(t_{m-1}, X_i^{m-1}) \\ \begin{bmatrix} (k-m+1)^{\alpha+1} \\ -(k-m)^\alpha (k-m+1+\alpha) \end{bmatrix}. \end{cases} \quad (67)$$

We consider our system with fractal–fractional derivative with Mittag–Leffler kernel

$$\begin{cases} {}^{\mathrm{FFM}}_{t_0}D_t^{\alpha,\beta} x(t) = a_1(y - x + \xi x - W(w)x), \\ {}^{\mathrm{FFM}}_{t_0}D_t^{\alpha,\beta} y(t) = x - y + z, \\ {}^{\mathrm{FFM}}_{t_0}D_t^{\alpha,\beta} z(t) = -\beta_1 y - \gamma z, \\ {}^{\mathrm{FFM}}_{t_0}D_t^{\alpha,\beta} w(t) = x. \end{cases} \quad (68)$$

The estimation of the parameters of the model and initial data is considered as

$$\begin{gathered} x(0) = 0.001, \quad y(0) = 0.001, \quad z(0) = 0.001, \\ w(0) = 0.001, \quad a_1 = 13.4, \quad \xi = 1.4, \\ \beta_1 = 11, \quad \gamma = 0.2, \quad a = 0.2, \quad b = 0.4, \\ a_1 = 2.32, \quad b_1 = 0.24, \quad c_1 = 0.14. \end{gathered} \quad (69)$$

The numerical simulation for the model in the case of fractal–fractional derivative with Mittag–Leffler kernel is presented in Figure 7.

4 Conclusion

In this study, we analyzed a modified memristor system using piecewise memductance functions and fractal–fractional derivatives with various kernels. Our findings indicate that the memristor exhibits chaotic behavior, confirmed through equilibrium point, stability, dissipativity,

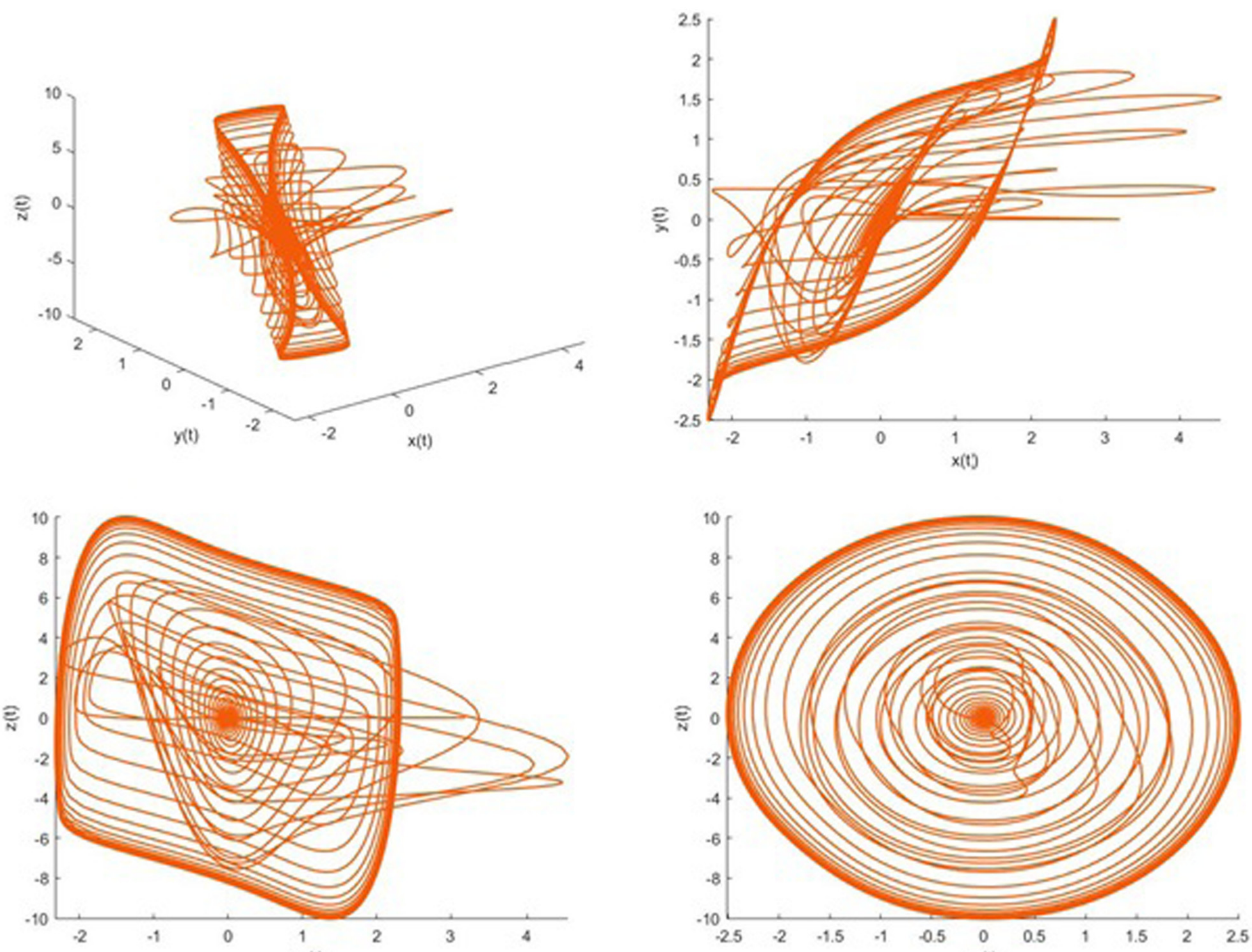

Figure 6: The graphical representation of the chaotic behavior of the fractal–fractional memristor system with piecewise memductance for $\alpha = 0.99$; $\beta = 0.99$.

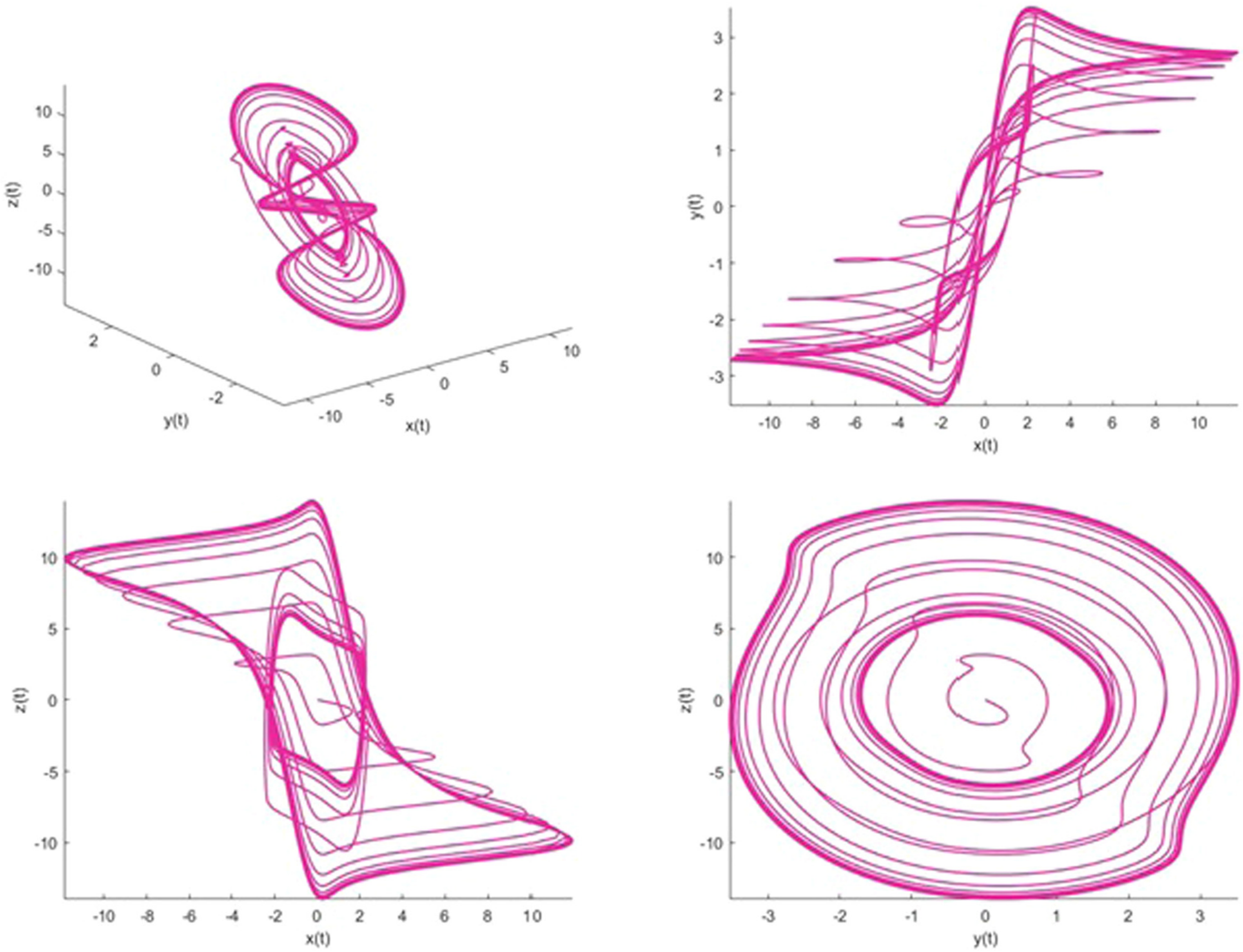

Figure 7: The graphical representation of the chaotic behavior of the fractal–fractional memristor system with piecewise memductance for $\alpha = 0.99$; $\beta = 0.99$.

and Lyapunov exponent analyses. The existence and uniqueness of this model is proved by employing Banach and Krasnoselskii fixed-point theorem. Numerical simulations demonstrated the dynamic responses of the memristor under classical and fractal–fractional derivative conditions. The proposed models and simulations enhance the understanding of memristor dynamics, providing a foundation for future applications in computing and electronics. These results contribute to the development of more accurate and reliable memristor-based systems.

The future direction of this work involves incorporating fractals by utilizing fractal-based circuit components in the modeling of resistive elements. Additionally, the resistive switching behavior could be modeled using fractal time series or stochastic processes. This approach aims to better capture the complex, self-similar nature of resistive switching phenomena, providing a more accurate and nuanced representation of the behavior in various systems. By integrating fractals, the work could improve the understanding and simulation of resistive switching in advanced materials and devices.

Funding information: The authors state no funding involved.

Author contributions: Seda Igret Araz: conceptualization, investigation, methodology, software, supervision, visualization, writing – review and editing. Maroua Amel Boubekeur: conceptualization, investigation; visualization; roles/writing – original draft; writing – review and editing. Irem Akbulut Arık: conceptualization, investigation, visualization, roles/writing – original draft, writing – review and editing. All authors have accepted responsibility for the entire content of this manuscript and approved its submission.

Conflict of interest: The authors state no conflict of interest.

Data availability statement: All data generated or analysed during this study are included in this published article.

References

[1] Doungmo-Goufo EF, Khan Y. The fractional and piecewise structure of some chaotic neural networks using a generalized model. Fractals. 2022;30(8):2240228.
[2] Doungmo-Goufo EF. The Proto-Lorenz system in its chaotic fractional and fractal structure. Int J Bifurcat Chaos. 2020;30(12):2050180.
[3] Abro KA, Memon IQ, Yousef A, Al-Mdallal QM. A comparative analysis of fractal and fractionalized thermal non-equilibrium model for chaotic convection saturated by porous medium. South Afr J Chem Eng. 2025;51:124–35.
[4] Bao BC, Liu Z, Xu JP. Dynamical analysis of memristor chaotic oscillator (in Chinese). Acta Phys Sin. 2010;59(6):3785–93.
[5] Apollos E. Memristor theory and mathematical modelling. Int J Comput Appl. 2019 Jun;178(27):1–8.
[6] Radwan AG, Zidan MA, Salama KN. On the mathematical modeling of memristors. In 2010 International Conference on Microelectronics. Vol. 19. 2010. p. 284–7.
[7] Elgabra H, Farhat IA, Al Hosani AS, Homouz D, Mohammad D. Mathematical modeling of a memristor device. In :2012 International Conference on Innovations in Information Technology (IIT). Vol. 18. 2012, p. 156–61.
[8] Abro KA, Atangana A. Mathematical analysis of memristor through fractal-fractional differential operators: a numerical study. Math Methods Appl Sci. 2020;43(10):6378–95.
[9] Sun J, Yao L, Zhang X, Wang Y, Cui G. Generalised mathematicalmodel of memristor. IET Circuits Devices Syst. 2016;10(3):244–9.
[10] Bao BC, Shi GD, Xu JP, Liu Z, Pan SH. Dynamics analysis of chaotic circuit with two memristors. Sci China Tech Sci. 2011;54:2180–7.
[11] Zhou L, Wang C, Zhou L. Generating hyperchaotic multi-wing attractor in a 4D memristive circuit. Nonl Dyn. 2016;85:2653–63.
[12] Ainamon C, Chamgoué AC, Kingni ST, Yamapi R, Orou JBC, Woafo P. Memristor Helmholtz oscillator: analysis, electronic implementation, synchronization and chaos control using single controller. In: Mem-elements for Neuromorphic Circuits with Artificial Intelligence Applications. United Kingdom: Elsevier; 2021. p. 207–23.
[13] Atangana A. Fractal-fractional differentiation and integration: connecting fractal calculus and fractional calculus to predict complex system. Chaos Solitons Fractals. 2017;102:396–406.
[14] Chen W. Time-space fabric underlying anomalous diffusion. Chaos Solitons Fractals. 2006;28:923–9.
[15] Caputo M. Linear model of dissipation whose Q is almost frequency independent. II. Geophys J Int. 1967;13(5):529–39.
[16] Caputo M, Fabrizio M. On the notion of fractional derivative and applications to the hysteresis phenomena. Mechanica. 2017;52(13):3043–52.
[17] Atangana A, Baleanu D. New fractional derivatives with non-local and non-singular kernel. Theory Appl Heat Transfer Model Thermal Sci. 2016;20(2):763–9.
[18] Krasnoselskii MA, Krein SG. On a class of uniqueness theorems for the equation $y' = f(x, y)$. Usphe. Mat. Nauk (N.S) 1956;11(1):209–13. (Russian:Math. Rev. 18, p. 38)
[19] Wolf A, Swift J, Swinney HL, Vastano J. Determining Lyapunov exponents from a time series. Phys D Nonl Phenomena. 1985;16(3):285–317.
[20] Bhaskar TG, Lakshmikanthama V, Leela S. Fractional differential equations with a Krasnoselskii-Krein type condition. Nonlinear Anal Hybrid Sys. 2009;3:734–7.
[21] Wu J, Liu Y. Uniqueness results and convergence of succesive approximations for fractional differential equations. Hacettepe J Math Stat. 2013;42(2):149–58.
[22] Atangana A, Igret Araz S. Step forward on nonlinear differential equations with the Atangana-Baleanu derivative: Inequalities, existence, uniqueness and method. Chaos Solitons Fractals. 2023;173:113700.
[23] Sudsutad W, Thaiprayoon C, Kongson J, Sae-dan W. A mathematical model for fractal-fractional monkeypox disease and its application to real data. AIMS Math. 2024;9(4):8516–63.
[24] Mekkaoui T, Atangana A. New numerical approximation of fractional derivative with non-local and non-singular kernel: Application to chaotic model. Europ Phys J Plus. 2017;132:444.